







where  $\lambda$  is the incident light wavelength,  $K$  is the Kerr constant,  $(\Delta n)_o$  is the maximum induced birefringence, and  $E_s$  is the saturation field. It is known that Kerr effect holds only in the low field region. As the electric field keeps on increasing, the induced birefringence would gradually saturate [17]. Unless specifically mentioned, throughout our simulations we assume  $K = 12.7 \text{ nm/V}^2$  and  $(\Delta n)_o = 0.2$  at  $\lambda = 550 \text{ nm}$ . After we have obtained the birefringence distribution, we apply extended Jones matrix methods to calculate the electro-optical properties [18,19]. In order to achieve low operating voltage and high transmittance, the parameters of the protrusion electrode are optimized at:  $w_1 = 0.5 \mu\text{m}$ ,  $w_2 = 1 \mu\text{m}$ ,  $h = 2 \mu\text{m}$ ,  $l_T = 2 \mu\text{m}$ , and  $l_R = 3 \mu\text{m}$ . And the optimized biaxial film has  $N_z = (n_x - n_z)/(n_x - n_y) = 0.5$ .

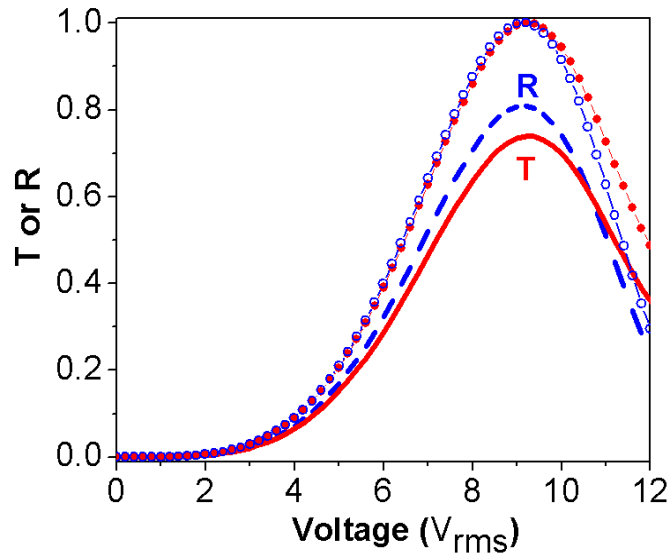


Fig. 2. Simulated VT and VR curves for the proposed transfective BP LCD. The solid red and dashed blue lines represent simulated VT and VR curves, and the closed circles and open circles represent normalized transmittance and reflectance.

Figure 2 shows the simulated VT and VR curves at  $\lambda = 550 \text{ nm}$ , both of which are normalized to the transmittance of two parallel polarizers (34.83%). Red curve (solid line) represents the transmittance, with a peak of  $\sim 74\%$ , and blue curve (dashed lines) represents the reflectance with a peak of  $\sim 81\%$ . Both T and R modes have a reasonably high optical efficiency. The on-state voltage for both regions occurs at  $\sim 9.2 \text{ V}_{\text{rms}}$ , thus this device can be addressed by amorphous-silicon thin film transistors (a-Si TFTs). The closed and open circles represent the normalized transmittance and reflectance, respectively. They overlap with each other quite well, which enables a single gamma curve driving.

Figures 3(a) and 3(b) depict the simulated isocontrast contour plots of the T and R regions, respectively. To take the color dispersion into account, in our isocontrast simulation, we assume the white light spectrum contains 60% green ( $\lambda = 550 \text{ nm}$ ), 30% red ( $\lambda = 650 \text{ nm}$ ), and 10% blue ( $\lambda = 450 \text{ nm}$ ). From Fig. 3, the averaged contrast ratio in the T region remains quite superb: the 1000:1 contrast ratio (CR) is over  $45^\circ$  viewing cone and 100:1 is over the entire viewing cone. In the R region,  $\text{CR} = 10:1$  is over  $50^\circ$ . These wide-view characteristics originate from the optically isotropic property of the BPLC.

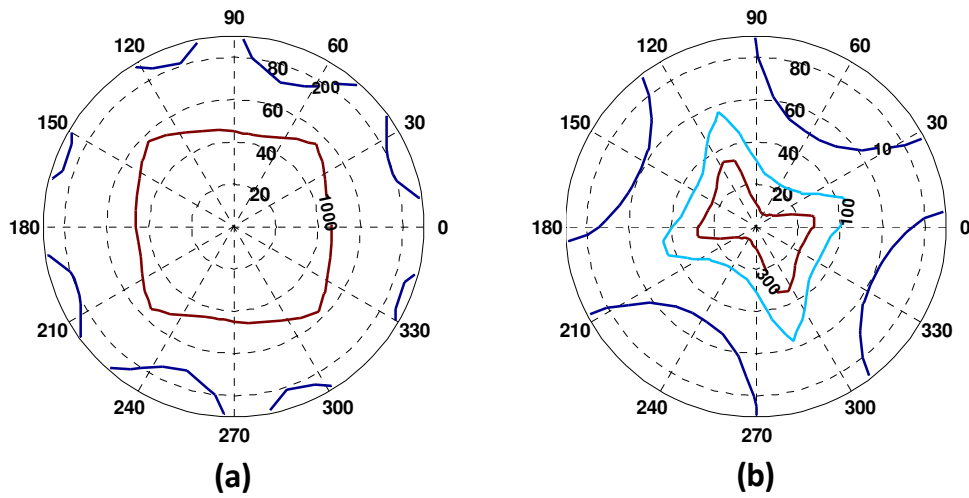


Fig. 3. Simulated isocontrast contour plots for (a) T mode and (b) R mode of the proposed TR-LCD.

For the proposed BPLC device, the operating voltage ( $\sim 9.2 V_{rms}$ ) is still higher than a conventional nematic LCD whose operating voltage is usually  $< 7 V_{rms}$ . Two approaches have been commonly taken to lower the operating voltage of BPLC devices: employing a large Kerr constant material, and optimizing the electrode configuration. Here we focus on improving the device configuration while keeping the Kerr constant at  $K = 12.7 \text{ nm/V}^2$  at  $\lambda = 550 \text{ nm}$  and room temperature ( $\sim 23^\circ\text{C}$ ) [20].

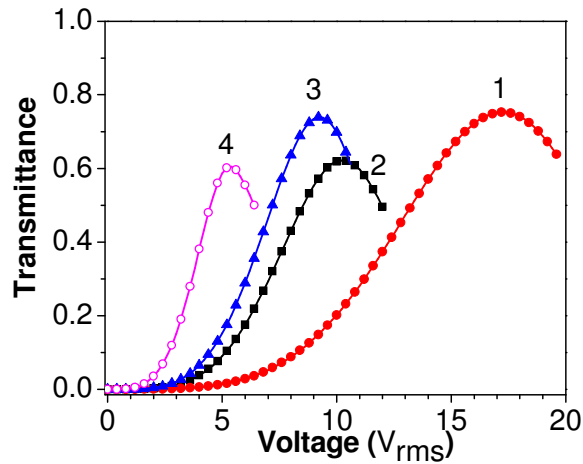


Fig. 4. Simulated VT curves with different protrusion-electrode device structures. 1)  $w_1 = 1 \mu\text{m}$ ,  $w_2 = 2 \mu\text{m}$ ,  $h = 2 \mu\text{m}$ , and  $l_T = 4 \mu\text{m}$ ; 2)  $w_1 = 1 \mu\text{m}$ ,  $w_2 = 2 \mu\text{m}$ ,  $h = 2 \mu\text{m}$ , and  $l_T = 2 \mu\text{m}$ ; 3)  $w_1 = 0.5 \mu\text{m}$ ,  $w_2 = 1 \mu\text{m}$ ,  $h = 2 \mu\text{m}$ , and  $l_T = 2 \mu\text{m}$ ; and 4)  $w_1 = 0.5 \mu\text{m}$ ,  $w_2 = 1 \mu\text{m}$ ,  $h = 2 \mu\text{m}$ , and  $l_T = 1 \mu\text{m}$ .

Figure 4 shows the simulated VT curves of four different electrode designs for T region. Curves 1 and 2 share the same protrusion shape ( $w_1 = 1 \mu\text{m}$ ,  $w_2 = 2 \mu\text{m}$ , and  $h = 2 \mu\text{m}$ ) but with different electrode gaps  $l_T$  ( $4\text{-}\mu\text{m}$  for curve 1 and  $2\text{-}\mu\text{m}$  for curve 2). As the electrode gap gets smaller, the peak voltage is reduced from  $\sim 17 V_{rms}$  to  $\sim 10 V_{rms}$ . However, the tradeoff is the lower transmittance (from  $\sim 75\%$  to  $\sim 63\%$ ). The decreased transmittance results from

increased ratio of dead zones as the electrode gap decreases. In an IPS structure, the dead zones occur at the middle of the electrodes. Curves 3 and 4 have a smaller protrusion dimension ( $w_1 = 0.5 \mu\text{m}$ ,  $w_2 = 1 \mu\text{m}$ , and  $h = 2 \mu\text{m}$ ) and a smaller electrode gap  $l_T$  ( $2\text{-}\mu\text{m}$  for curve 3 and  $1\text{-}\mu\text{m}$  for curve 4). The influence of gap variation as mentioned before stays true in the comparison of curves 3 and 4. Although curve 4 exhibits a very low operating voltage ( $\sim 5 \text{ V}_{\text{rms}}$ ), its transmittance is reduced to  $\sim 60\%$ . We also studied the effects of protrusion height (results are not shown here). Increasing the protrusion height is an effective way to reduce the operating voltage without sacrificing transmittance too noticeably. However, the fabrication of small and steep protrusion electrodes using current lithography remains a challenge. As the nanoimprinting technology advances, the fabrication of small dimension protrusion electrodes will no longer be a hurdle. Thus, the operating voltage could be further reduced, which is highly desirable for mobile display devices.

An important advantage of the proposed TR-LCD is its submillisecond gray-to-gray response time [9]. If the transmissive BP LCD employs spatial color filters, the inherent fast response time is helpful for reducing motion picture image blurs. Moreover, such a fast response feature enables color sequential mode in the T region with RGB LED backlight [3]. The removal of color filters would triple the optical efficiency and resolution density in the T region. In the R region, color filters are optional. Without color filters, the reflectance will be greatly enhanced except that the display will appear black and white. On the other hand, if color filters are employed in the R region, then its performance in reflective mode will be comparable to a typical nematic TR-LCD. If the LED backlight is kept on, then the total optical efficiency will still be superior to that of nematic TR-LCD.

#### 4. Conclusion

We have proposed a fast response, wide view, and single-cell-gap transmissive display based on polymer-stabilized BPLC. In such a cell no surface alignment layer is needed which simplifies the fabrication process. Both T and R regions of this TR-LCD exhibit a reasonably high optical efficiency. The VT and VR curves match very well which enables a single gamma curve driving. The viewing angle (under white light) for T mode is excellent, and for R mode is also adequate for mobile display applications. This is because the BPLC has an optically isotropic dark state. Moreover, its submillisecond response time would reduce the image blurs, and if field sequential operation is employed in T region its optical efficiency and resolution density are both tripled. As the nanoimprinting technology advances, the fabrication of protrusion electrodes will become easier. As a result, the proposed transmissive BP LCD has great potential for mobile display applications.

#### Acknowledgments

The authors are indebted to the financial support from ITRI, Taiwan.